ELSEVIER

Journal of Power Sources 108 (2002) 153–162

JOURNAL OF POWER SOURCES

www.elsevier.com/locate/jpowsour

Porous electrodes-based double-layer supercapacitors: pore structure versus series resistance

A. Celzard[a,*], F. Collas[a], J.F. Marêché[a], G. Furdin[a], I. Rey[b]

[a]*Laboratoire de Chimie du Solide Minéral, Université Henri Poincaré-Nancy I, UMR-CNRS 7555, BP 239, 54506 Vandoeuvre-lès-Nancy Cédex, France*

[b]*Bolloré Technologies, Odet, BP 607, 29551 Quimper Cédex 9, France*

Received 21 September 2001; received in revised form 17 December 2001; accepted 22 December 2001

Abstract

The correlation between the porous structure of electrodes designed for double-layer supercapacitors and the series resistances of the latter is addressed in this paper. It is shown that in such composite films, made of active carbon embedded in a porous polymer, the internal electrolyte resistance within the pores governs the series resistance. In order to evidence this, various compositions of polymer–carbon mixtures are manufactured. Their porosities are determined, both before and after impregnating them with the solvent of the electrolyte. For the compositions under study, the nature of the solvent is found to induce very different effects on the permeability of the films. However, the transport properties within the pore space of the composites are also investigated via ion diffusion experiments. Whatever the solvent, a strong correlation is found between formation factors of the porous films and the series resistances of the final double-layer supercapacitors.

Keywords: Supercapacitor; Series resistance; Porosity; Formation factor; Permeability; Diffusion

1. Introduction

It is well known that the power output capability of electrical capacitors depends strongly on the series resistance R_s, which needs to be minimised [1]. For supercapacitors made of high-area porous materials either made of carbon matrices or containing powdered carbon invaded by a suitable electrolyte, the contributions to the absolute value of R_s are manyfold. Indeed, R_s is the sum of two major terms, namely an electronic contribution and an ionic one. The former comprises intrinsic electrical resistivity of the dispersed carbon grains, and both grains-to-grains and grains-to-current-collector contact resistances, while the latter concerns the resistivity of the electrolyte within the pores. Minimising all these terms leads to the maximum power performance of the supercapacitor.

However, other parameters were experimentally found to enhance the series resistance, especially the increase of the percentage of active carbon and that of the electrode thickness. Such features are rather striking, since the electrical resistivity along the film decreases as the filler content and the film thickness increase. Besides, the series resistance depends on the solvent of the electrolyte impregnating the electrode. These findings suggest that the ionic contribution introduced above, rather than the electronic one, is involved in such phenomena. The aim of the present paper is to give experimental evidence of this interpretation.

For that purpose, the investigation of the pore structure of some composite electrodes is worth performing. Especially, the so-called formation factor F and the tortuosity τ are known to be very useful parameters characterising the pore space [2]. They are such that:

$$\tau = FP, \tag{1}$$

where P is the throughout porosity of the medium, and F is defined by the following ratios:

$$F = \frac{\sigma_0}{\sigma} = \frac{D_0}{D}, \tag{2}$$

where σ_0 is the ionic conductivity of a pure electrolyte and σ that of the material which pore space is saturated with the same electrolyte. D_0 represents the diffusion coefficient of the electrolyte ions in a given solvent, and D corresponds to that of the same ions diffusing in the pore space of the material saturated with the same solvent.

* Corresponding author. Tel.: +33-3-83-91-21-87; fax: +33-3-83-91-25-68.
E-mail address: alain.celzard@lcsm.uhp-nancy.fr (A. Celzard).

0378-7753/02/$ – see front matter
PII: S0378-7753(02)00030-7

Then, if pores are non intersecting tortuous cylinders, the tortuosity is the ratio of the mean diffusion path length (Λ) to the sample thickness (L). If the capillary tubes intersect, the measured tortuosity is always greater than Λ/L; τ, thus, appears to be an empirical coefficient accounting for the random orientation of the pores within the material [3]. Practically, tortuosities are calculated from Eqs. (1) and (2), and from the experiments leading to the corresponding factors F. In the following, the solvent-impregnated electrodes will indeed be investigated in this way. Since these materials comprise a high carbon content, they are very conducting and, hence, F is measured by ion diffusion experiments. However, F and thus τ may also be derived from permeability and mercury porosimetry data.

Electrode films made of active carbon embedded in porous polymers are described in this article. Their porous structure is investigated both before and after impregnation with the solvent of the electrolyte. In Section 2, dc electrical conductivity, fluid permeability of films both as-produced and subsequently immersed in a solvent, and diffusion coefficients of ions in solvent-wetted electrodes are measured. The results are discussed in Section 3; a model of pore structure is proposed both for dry and wet films, and the formation factors are calculated in each case. A correlation between F and the series resistance R_s is finally evidenced. R_s is shown to be an increasing function of F for both solvents, although the corresponding composites have very different pore structures.

2. Experimental

2.1. Porous electrodes

The supercapacitor electrodes are, as usual in such devices, thick composite films made of active carbon grains embedded in a porous polymer matrix. For the present investigation, six different compositions having different carbon contents and porosities are processed. These materials were especially prepared for the present study, but their composition is relevant since it is typical of actually working electrodes for supercapacitors. The samples are referred as F_1–F_6 and their main characteristics are given in Table 1. They are such that the weight of the carbon to that of the polymer is always constant. On the one hand, active carbon grains are required because of both their electrical conductivity and their high surface area. On the other hand, porosity all throughout the materials allows the accessibility of a given electrolyte to this surface, leading to high double-layer capacities. It should be emphasised that the chemical nature of the porous polymer as well as the origin of the active carbon are absolutely not crucial in the following study. Indeed, as shown below, only purely physical mechanisms are involved. Hence, the concerned processes should be encountered in any other other kind of porous electrode comprising active carbon grains. The porosities of the films were derived from mercury intrusion experiments (see below) and are presented in Table 1.

Table 1
Main characteristics of the six composite films (called F_1–F_6) investigated here

Sample	Active carbon (wt.%)	P_{dry} (vol.%)	$P_{aceto.}$ (vol.%)	$D_{aceto.}$ ($cm^2\ s^{-1}$)	$D_{\gamma\text{-but.}}$ ($cm^2\ s^{-1}$)
F_1	53.6	21.7	15.1	2.9×10^{-7}	5.9×10^{-8}
F_2	53.7	23.3	16.2	3.9×10^{-7}	–
F_3	53.0	24.2	16.9	4.3×10^{-7}	8.0×10^{-8}
F_4	53.1	25.9	18.1	3.0×10^{-7}	8.7×10^{-8}
F_5	51.6	27.8	19.4	5.2×10^{-7}	–
F_6	51.7	31.2	22.2	7.2×10^{-7}	9.1×10^{-8}

P_{dry}: the porosity of the materials in the dry state, i.e. not wetted by any solvent. $P_{aceto.}$: the residual porosity after impregnation of the films with acetonitrile. $D_{aceto.}$ and $D_{\gamma\text{-but.}}$: the diffusion coefficients of KSCN within the materials wetted either by acetonitrile or γ-butyrolactone, respectively.

The electrical resistivity ρ of the porous films is measured both along their basal plane ($\rho_{//}$) and across their thickness ($\rho\perp$) by a four-probe method. A low anisotropy is evidenced, as shown in Fig. 1. Concurrently, the series resistances R_s of supercapacitors made of such electrodes impregnated by an electrolyte dissolved in two different solvents are measured. The latter are such that they both possess a high dielectric constant and are not decomposed by the voltage. Many examples of such solvents may be found in [1]. Thus, acetonitrile and γ-butyrolactone were chosen for the present study. Indeed, these solvents are both convenient for their application in supercapacitors and have very different viscosities. For measuring the series resistance, the output voltage is analysed as a function of time at the very beginning of the discharge of the supercapacitor

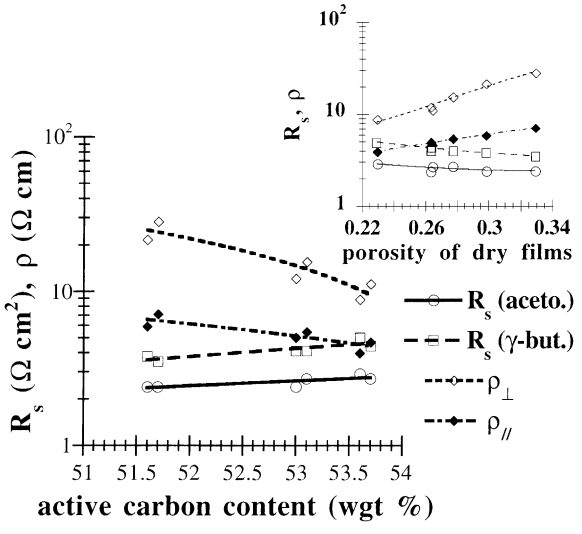

Fig. 1. Electrical resistivity ρ of porous polymer—active carbon composite electrodes before impregnating them with a solvent, as a function of their weight content of carbon. The parameter $\rho_{//}$ is the resistivity measured parallel to the direction of extrusion, while $\rho\perp$ is that measured across the thickness. Series resistances R_s of supercapacitors made of such porous electrodes impregnated with either acetonitrile (aceto.) or γ-butyrolactone (γ-but.). Solid and broken curves are just guides for the eye.

through a resistor. The corresponding data are also presented in Fig. 1. It is seen that R_s is an increasing function of the active carbon content, while ρ decreases. Such a behaviour is only paradoxal if the purely electronic part of the resistances is considered. Moreover, the range of carbon content is very narrow and hence cannot explain such differences in both intrinsic resistivities and series resistance. Rather, the prevalence of the ionic contribution is suggested as soon as R_s and ρ are plotted as a function of the porosity, as shown in the inset of Fig. 1. Additionally, increasing the carbon content may lead to pores which are more and more tortuous across the thickness of the film, thus, hindering the ionic conductivity across the material impregnated with its electrolyte. Besides, increasing the film thickness induces the same effect. Hence, it seems that the resistance of a given electrolyte within the pores is the major contribution to R_s; the nature of the conductive filler dispersed in the polymer matrix is, thus, probably not a crucial parameter. More exactly, it is suggested in the following that the formation factors of the porous films are strongly correlated to the series resistances, as far as identical solvents and electrolytes are considered.

Preparation of a double-layer supercapacitor requires the winding of a pair of films (with their current-collectors) accompanied with a suitable separator. The resulting block is then kept in a constrained state into a rigid cylindrical container, and next impregnated with an electrolyte dissolved in a solvent. As written above, two solvents are considered here, which both make the films swell considerably in a reversible way. Indeed, the resistivity of porous electrode films immersed either in acetonitrile or in γ-butyrolactone strongly increases, then stabilises within a few minutes, and finally decreases down to its initial value as soon as the materials are dried [4]. Such swelling phenomena are well known in polymer materials, and some conducting polymeric composites were suggested to be used as chemical sensors, basing on such a mechanism [5]. Thus, for example, the resistivity of F_4 is multiplied by factors of about 50 and 200 in acetonitrile and γ-butyrolactone, respectively. However, these phenomena are not exactly those encountered in actual supercapacitors, since the electrodes are impregnated with solvent in a constrained state. Such a situation was simulated by wetted films which were not completely allowed to swell, by first pressing them firmly between two highly porous pieces of sintered ceramic and next soaking them into solvent. It has been observed that the magnitude of the increase in electrical resistance in such a case was much lower, ρ being multiplied by 10 and by 20 in acetonitrile and γ-butyrolactone, respectively. These findings mean that the spreading out of the conducting carbon grains was considerably hindered. Nevertheless, the swelling of the polymeric matrix yet occurred, certainly at the expense of the initial porosity as it is shown below. In Section 3, the shrinkage of the pore structure and the corresponding increase of the formation factors is indeed evidenced.

2.2. Permeability

The fluid permeability k of the materials is worth measuring for quantifying the phenomena described above. Thus, as discussed in Section 3, the gas permeability brings informations about the pore structure of the dry electrodes, i.e. before being included in a supercapacitor. However, as solvent-induced modifications of the porosity are suspected, it appears that permeability measurements of the electrodes in actual working conditions, i.e. swelled by solvent in an almost undeformable volume, are also required. Indeed, the behaviour of the wet films is somewhat different, depending on the nature of the impregnating solvent. In acetonitrile, the materials curl and are still permeable although k strongly decreases (see below), while in γ-butyrolactone, the swelling leads to a kind of polymeric gel, in which no permeability is measurable. It should be noticed that for both dry and wet films, the permeability brings information about the throughout porosity of the films. Therefore, the ''blind'' narrow porosity of the carbon grains is not concerned by such experiments. Moreover, the permeability is a physical quantity controlled by the largest and the most connected pores, i.e. those of the polymeric material. Thus, permeability measurements are of interest since the concerned porosity is also expected to control the diffusion processes and, hence, the series resistance of the resultant supercapacitor.

Two kinds of measurements are thus made, either with a gas (nitrogen) for dry films, or with a solvent (acetonitrile or γ-butyrolactone) for wet films. In the first case, a sample is installed as a membrane throughout which nitrogen is forced to span with various inlet pressures P_1. During each experiment, P_1 is maintained constant, while both the flow rate Q and the pressure drop $\Delta P = P_1 - P_2$, (P_2 being the outlet pressure), are simultaneously measured (see Fig. 2a). In the second case, the porous film is a membrane tightly maintained between two rigid thin metallic grids and throughout which the solvent is allowed to flow. The pressure of the liquid is kept constant by continuously adjusting the column height Z at a constant value (see Fig. 2b), and the outlet volume of solvent is measured after a given time.

The calculation of the corresponding permeabilities is based on application of Darcy's law [6,7], which reads:

$$k = Q\frac{L}{S}\left(\frac{\eta}{P_1 - P_2}\right), \tag{3}$$

for a liquid, i.e. an incompressible fluid, and

$$k = -Q\frac{L}{S}\eta\left[\frac{2(P_1 - \Delta P)}{(P_1 - \Delta P)^2 - P_1^2}\right], \tag{4}$$

for a compressible fluid, like a gas. In these equations, k is the permeability of the porous medium, η the dynamic viscosity of the fluid, L the thickness of the sample, S its cross-sectional area, Q the flow rate of the fluid and $\Delta P = P_1 - P_2$ is the pressure drop over the sample. In Eq. (3),

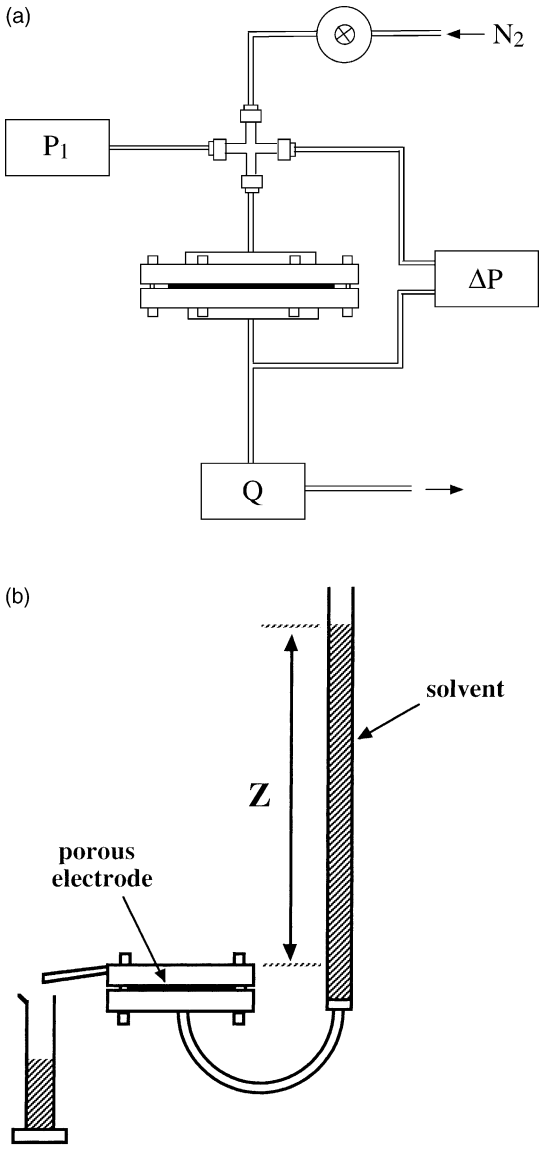

Fig. 2. Schematical view of the devices with which the permeabilities are measured. (a) Gas permeability of dry electrodes. The porous film is a membrane throughout which nitrogen is forced to flow. Inlet pressure P_1, pressure drop ΔP and flow rate Q are simultaneously measured; (b) liquid permeability of solvent-impregnated electrodes. The height Z of the column of solvent is kept constant all along the experiment, and the volume of liquid passing throughout the porous film is measured after a given time.

$\Delta P = ngZ$, where g is the gravitational acceleration (9.81 m s^{-2}), and n the density of the fluid, i.e. 0.786 and 1.13 g cm^{-3} for acetonitrile and γ-butyrolactone, respectively [8]. The dynamic viscosity at 25 °C is 17.9 μPa s for nitrogen, while those of acetonitrile and γ-butyrolactone are 0.3 and 1.7 mPa s, respectively [9]. Parameter k has the unit of an area, and is often expressed in millidarcies (mD), where 1 mD $\approx 10^{-15}$ m^2.

The results are shown in Fig. 3, in which the permeabilities of dry electrodes (i.e. measured with nitrogen) and wet ones (measured with acetonitrile) are plotted. Although k is

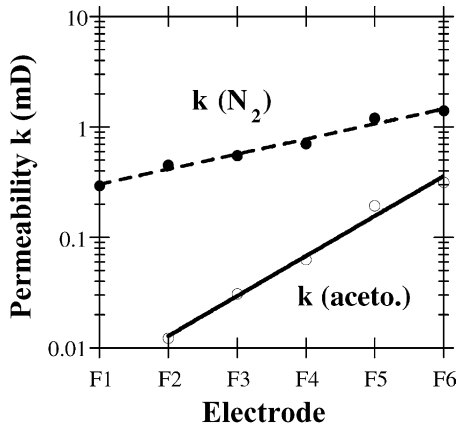

Fig. 3. Permeabilities k of both dry materials (measured with flowing nitrogen, see Fig. 2a) and solvent-impregnated materials (measured with flowing acetonitrile, see Fig. 2b). The solid lines interpolate the experimental data; $k \approx 0$ in γ-butyrolactone, whatever the samples.

lowered due to the decrease of the porosity in the case of films impregnated with acetonitrile, it can be seen that the behaviour of the permeabilities is qualitatively the same for both dry and wet electrodes. Conversely, no flow of liquid has been evidenced throughout materials impregnated with γ-butyrolactone.

The fact that $k \approx 0$ in materials wetted with γ-butyrolactone does not mean that the ions of the electrolyte are no more able to move inside the films. Rather, this signifies that viscous flow is totally replaced by diffusional processes. Hence, diffusivity of ions throughout the wetted electrodes is another worth measuring useful parameter. Indeed, formation factors may be derived from such measurements.

2.3. Ion diffusion experiments

The diffusion coefficients of ions in wetted films are measured via a conductimetric method. Potassium thiocyanate (KSCN), rather than an actual electrolyte operating in supercapacitors, is the salt with which the experiments are made. The reason of such a choice lies on the fact that the ions K^+ and SCN^- possess diffusion coefficients which are close to each other. Besides, KSCN both may be handled without particular cares and is soluble in the two solvents. Conversely, the electrolytes actually introduced in supercapacitors are much more expensive and usually highly moisture sensitive, and thus, needs to be handled inside a glove box.

The measurement cell has the classical structure illustrated in Fig. 4. The electrode is kept between two pieces of highly porous sintered ceramics and constitutes a membrane separating two compartments. The first one (at the right of the figure, referred as no. 1) contains the solvent in which KSCN is dissolved at a concentration of 0.5 mol l^{-1}, while the second one (at the left, referred as no. 2) is filled with pure solvent. Both compartments are stirred with appropriate magnetic devices, and the conductivity of part

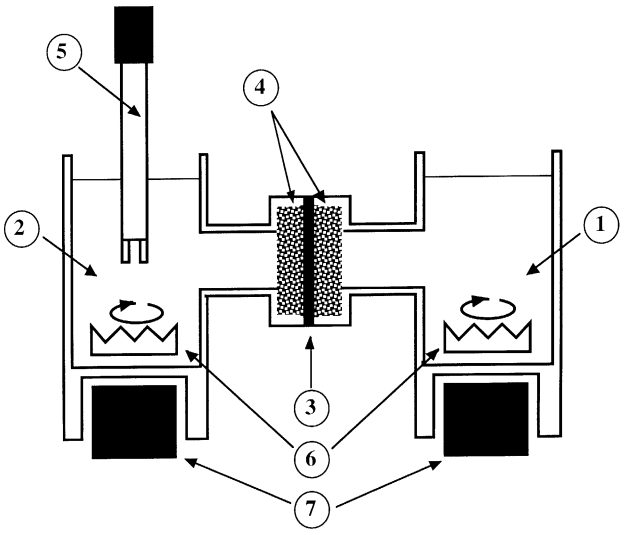

Fig. 4. Schematical view of the device with which the diffusion experiments are performed. Two compartments are separated by the electrode (3) which is held between two pieces of highly porous sintered ceramic (4). The first compartment (1) initially contains KSCN dissolved in solvent at a concentration of 0.5 mol l^{-1}, while the second one (2) is filled with pure solvent. The ionic conductivity in (2) is measured as a function of time using a four poles electrode cell (5). Both compartments are stirred with appropriate magnetic bars (6) rotated by small electric motors (7).

no. 2 is continuously recorded as a function of time. In order to determine the growing concentration of KSCN originating from the diffusion throughout the electrode, a calibration curve is established. For that purpose, the conductivities of a number of solutions of acetonitrile and γ-butyrolactone containing various amounts of dissolved salt are measured at 25 °C, as shown in Fig. 5a. It is seen that the ratio of the ionic conductivity in acetonitrile to that in γ-butyrolactone is roughly equals to 3.5, whatever the concentration of the salt. It is very likely that such a constant ratio is only due to the different viscosities of the solvents, since their relative dielectric constants are high and close to each other. Hence, similar dissociations are expected for any electrolyte.

The concentrations of KSCN in compartment 2 are then subsequently plotted as a function of time in Fig. 5b. After an initial delay t_0, during which diffusion of the ions becomes established across the thickness of the sample, there is a linear increase with time in the concentration of the solution in compartment 2. The diffusion coefficient is defined as the constant D in Fick's first law:

$$J = -D\frac{\mathrm{d}C}{\mathrm{d}x}, \tag{5}$$

where J is the flux of diffusing species in moles per time per unit of cross-sectional area, C their concentration, and $\mathrm{d}C/\mathrm{d}x$ the applied concentration gradient. Eq. (5) may be written as

$$\frac{V}{S}\frac{\mathrm{d}C_2}{\mathrm{d}t} = D\frac{C_1 - C_2}{L}, \tag{6}$$

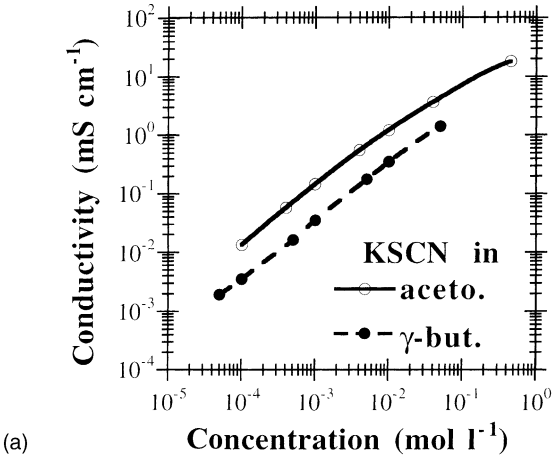

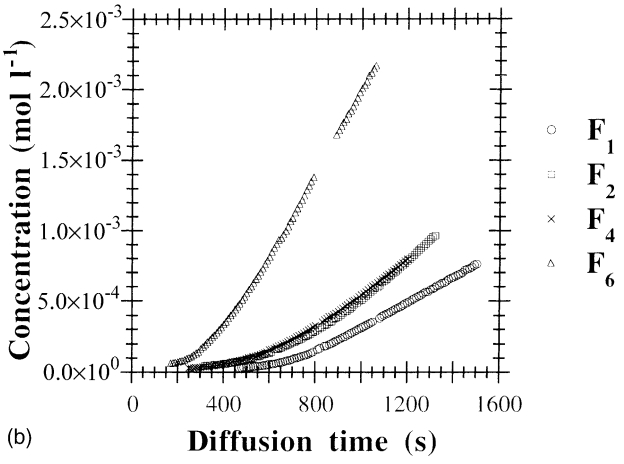

Fig. 5. (a) Calibration curves showing the changes of ionic conductivity of KSCN as a function of its concentration in both solvents; (b) typical plots of C_2 vs. the diffusion time t (in acetonitrile), where C_2 is the concentration of the ions in compartment (2) of Fig. 4. C_2 is calculated from the calibration curves given in Fig. 5a.

where S and L have the same meaning as before, V is the volume of solution in compartment 2, and C_1 and C_2 the solution concentrations, assumed to be equal to the activities, in parts 1 and 2 of the diffusion cell, respectively. Hence,

$$D = \frac{VL}{SC_1}\frac{C_2}{t - t_0}, \quad \text{if } C_2 \ll C_1. \tag{7}$$

Thus, the linear behaviours observed in Fig. 5b for diffusion times greater than t_0, which values depend both on the composition and on the thickness of the material, are accounted by Eq. (7). The effective diffusion coefficients within the materials are given in Table 1. Note that a few data are lacking for materials impregnated with γ-butyrolactone. The reason lies on the fact that irreproducible results were obtained, probably owing to the occurrence of microcracks induced by the handling of the films. The latter have indeed very poor mechanical properties on swelling by γ-butyrolactone.

2.4. Mercury porosimetry experiments

In Section 3, a model is introduced which states that the permeability is controlled by the critical pore diameter δ_c at which the mercury first percolates throughout the material. Porosimetry are thus needed for two reasons. First, basing on this model, it becomes possible to investigate the pore structure. Next, the porosities of the films (see Table 1) may be calculated from the porosimetry results.

Porosimetry experiments were performed on each material from F_1–F_6. Such a method is widely used to give informations about the approximative pore volume and distribution within porous media. For that purpose, hydrostatic pressure is increased from 0 up to 2070 bars according to an equilibration mode which allows mercury to flow into the pores for a specified length of time. The data output is the intruded volume as a function of applied pressure.

Raw injection curves are given in Fig. 6. As discussed below, and similarly to what is supposed in most porous materials, cylindrical pores are assumed. Such an assumption allows to apply the well-known Washburn equation [10], which assigns a particular pore diameter d to a given injection pressure p:

$$p = -\frac{4\gamma\cos\theta}{d}, \tag{8}$$

where θ is the contact angle between mercury and the material, and is assumed to be 130°, while $\gamma = 485$ dyn cm^{-1} is the surface tension of mercury.

It should be pointed out that the porosities obtained from this method do not take into account the microporosity of the carbon grains, which is responsible for the greatest part of the surface area. The smallest pores reached by mercury have indeed diameters close to 6 nm, as given straightforwardly by numerical application of Eq. (8) for the highest available pressure. The cumulative intruded volume of mercury per gram of porous sample is measured for each electrode, and the corresponding porosities are given in Table 1.

3. Discussion

3.1. Porosity and pore structure derived from permeabilities

3.1.1. Dry electrodes

Basing on percolation theory, it is easy to check that the permeabilities and the porosimetry data are consistent with each other. Indeed, the composite materials presented in this paper are highly and randomly disordered. Since the permeability of the dry films is known to be zero for porosities lower than $P_c \approx 15\%$ [4], a percolation-type behaviour is thus expected, such that [11]:

$$k \sim (P - P_c)^e, \quad P \to P_c, \tag{9}$$

where P_c is the critical porosity, i.e. the value of P below which the material becomes impermeable, and e is an exponent which value is close to 2 in any three-dimensional classical system [11]. The plot of log k versus log $(P - 0.15)$ is shown in Fig. 7. A straight line is indeed obtained, having a slope (1.835) in perfect agreement with the expected value for the critical exponent e.

Formation factors and tortuosities of dry materials may now be derived from both permeability and porosimetry data. Indeed, since k has the dimension of an area, it may be written as $k \sim \delta^2/F \sim P\,\delta^2/\tau$, where δ is a characteristic pore diameter. According to Katz and Thompson [12,13], such a length scale may be obtained from mercury intrusion experiments. In these conditions, δ is the critical pore diameter δ_c at which the invading mercury first forms a connected path spanning the sample. It may, thus, be seen as a percolation threshold in terms of pore diameter, and corresponds to a critical pressure of intrusion p^*. It has been first suggested

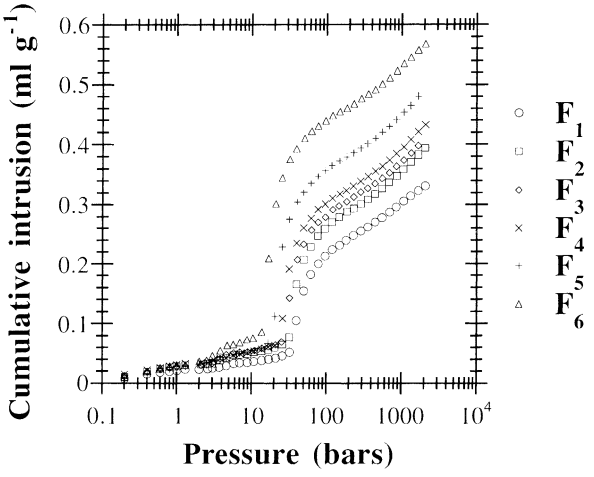

Fig. 6. Mercury injection capillary pressure curves for dry porous electrodes.

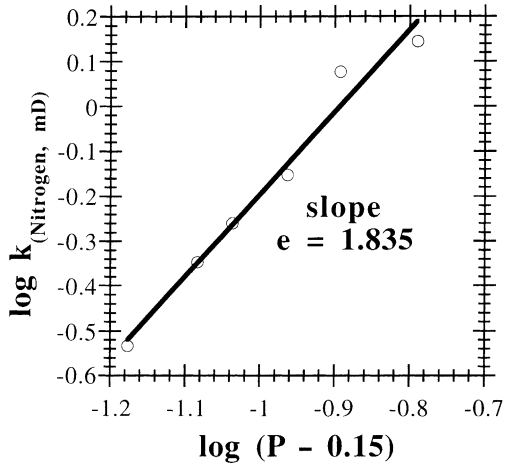

Fig. 7. Checking of Eq. (9) derived from percolation theory, in which the critical porosity is 15 vol.%. The slope of the straight line is in fair agreement with the expected value of the critical exponent e, i.e. close to 2.

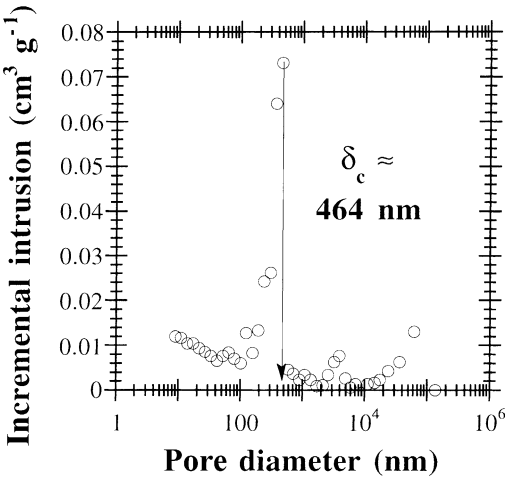

Fig. 8. Incremental volume of mercury intruded inside the film F_3 as a function of the pore diameter calculated according to Washburn's Eq. (8). Parameter δ_c is the characteristic pore diameter at the continuity threshold in mercury injection. A same kind of curve is obtained in the other materials.

[14,15] and later shown from resistivity measurements [16] that such a critical pressure coincides with the inflection point of the mercury injection curve, and hence, to the maximum of its derivative. In other words, δ_c is the abscissa of the maximum of the typical curve incremental intruded volume versus pore diameter. A typical result is presented in Fig. 8, in which the sample F_3 is shown to have a critical pore diameter of 464 nm. The values of δ_c for the other materials are gathered in Table 2.

Katz and Thompson theory states that:

$$k = C\frac{\delta_c^2}{F}, \tag{10}$$

where C is a constant depending on the pore structure. Therefore, F and thus τ are calculable if the relevant value of C is known. Several models considering cylindrical pores having wide distributions of diameters, but various lengths (see [17] for details) were tried, and only two of them were found to deserve attention. Indeed, as shown below, the latter lead to results which both are similar and have a physical meaning, since the calculated tortuosities are found to be >1, whatever the material.

Table 2
Critical pore diameters δ_c derived from mercury porosimetry experiments for each dry electrode (example given in Fig. 8)

Sample	δ_c (μm)	$l = l_0$		$l = \sqrt{r\delta}$		Average	
		F	τ	F	τ	F	τ
F_1	0.462	12.29	2.67	10.77	2.34	11.53	2.50
F_2	0.463	8.03	1.87	7.04	1.64	7.53	1.76
F_3	0.464	6.60	1.60	5.78	1.40	6.19	1.50
F_4	0.469	5.28	1.37	4.62	1.20	4.95	1.28
F_5	0.581	4.76	1.32	4.17	1.16	4.47	1.24
F_6	0.888	9.53	2.97	8.35	2.60	8.94	2.79

F and τ: the formation factors and the tortuosities calculated from Eqs. (1) and (10), respectively, in the framework of the two pore models ($l = l_0$ and $l = \sqrt{r\delta}$) considered in the text.

In the first model, the pores are cylinders having a constant length $l = l_0$, and which diameters δ are widely distributed (e.g. the distribution is log-normal). In such a case, $C_I \approx 1.69 \times 10^{-2}$ [18]. The second model deals with sinuous tubes having both a curvature r such that $l = \sqrt{r\delta}$ and again a wide distribution of diameters. Then, $C_{II} \approx 1.48 \times 10^{-2}$ [18,19]. Application of Eqs. (1) and (10) with the experimental data obtained for dry films leads to the results given in Table 2. It is seen that the formation factor roughly varies from 11 down to 4 as the porosity increases, i.e. from sample F_1 to sample F_5 (sample F_6 is an exception to this behaviour). The tortuosities are rather low as compared with the values usually found in other materials (like sintered glasses, rocks, porous carbons, etc.) [3]. The capillary tubes inside the dry electrodes, thus, appear to be rather straight, since they seem to be only slightly greater than the thickness of the films. These findings evidence that the porosity of the polymer film is indeed under study, and not that of the embedded active carbon grains.

3.1.2. Electrodes impregnated with solvent

Impregnation of the electrodes with acetonitrile leads to permeabilities which are lower than those of dry materials, as shown in Fig. 3. Since the flow of this solvent is still possible throughout wetted films, except for that having the lowest initial carbon content (F_1: $k \to 0$), the resulting porosity P' is obviously greater than P_c. Hence, Eq. (9) may be applied again, and it thus becomes possible to calculate P' for each film. For that purpose, log $k_{aceto.}$ versus log $(P - P'_c)$ is plotted in Fig. 9 for various values of P'_c until the best linear regression is obtained. The best correlation coefficient is found with $P'_c = 0.217$, for which a critical exponent ($e' = 1.833$) close to 2 is again obtained, see the

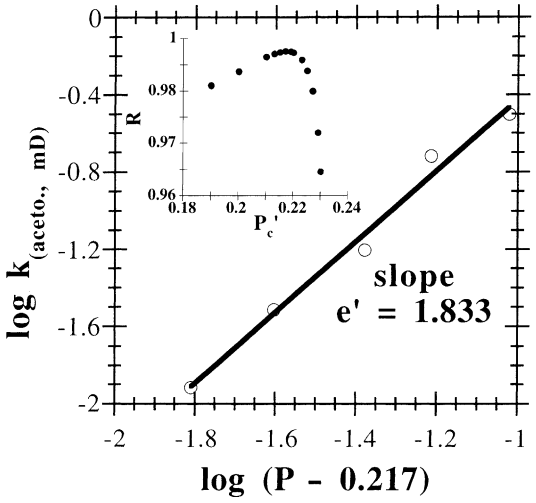

Fig. 9. Application of Eq. (9) for films impregnated with acetonitrile. The linear regression is obtained with a critical porosity $P'_c = 0.217$, as shown in the inset where the correlation coefficient R of the linear fits is plotted as a function of the trial values of P'_c.

Table 3
Equivalent ionic conductivities (λ) at 25 °C for K^+ and SCN^- dissolved in acetonitrile (values from [20]) and in γ-butyrolactone (estimated values, see text)

Solvent	λ_{K^+} (S cm^2 mol^{-1})	λ_{SCN^-} (S cm^2 mol^{-1})	D_{K^+} (cm^2 s^{-1})	D_{SCN^-} (cm^2 s^{-1})	D_{KSCN} (cm^2 s^{-1})
Acetonitrile	83.6	113.4	2.22×10^{-5}	3.02×10^{-5}	2.56×10^{-5}
γ-Butyrolactone	17	25	4.52×10^{-6}	6.65×10^{-6}	5.38×10^{-6}

The diffusion coefficients in both solvents are calculated from Eqs. (11) and (12).

inset of Fig. 9. This value of P'_c, hence, represents the porosity of the dry film which becomes impermeable with $P_{c(aceto.)} = 0.15$ after immersion in acetonitrile. The porosity of the impregnated materials may, thus, be estimated by $P_{aceto.} = P_{dry} \times 0.15/0.215$. The results are gathered in Table 1. It may be seen that the sample F_1 has a calculated porosity $P' = 0.151$, i.e. very close to the threshold P_c; this confirms the experimental finding that the permeability is about zero for this film.

The fact that no permeability is measurable in electrodes wetted by γ-butyrolactone indicates that the effective porosity for liquid flow, i.e. the volume fraction of capillary tubes, is always <15%. However, in such gels, porosity is ill-defined because a loose polymer network is formed rather than a matrix comprising true pores. Hence, estimating the porosity of films impregnated with γ-butyrolactone with the procedure used above in the case of acetonitrile can not be performed.

3.2. Pore structure derived from ion diffusion experiments (wet materials)

The values of D presented in Table 1 account for the simultaneous diffusion of both K^+ and SCN^- ions. These data now require to be compared with the diffusivities D_0 of the same salt in pure solvents. Thus, formation factors are obtained from the ratios D_0/D as dictated by Eq. (2). D_0 is related to the individual diffusion coefficients D_{K^+} and D_{SCN^-} by the following relationship:

$$D_0 = 2\frac{D_{K^+}D_{SCN^-}}{D_{K^+} + D_{SCN^-}}. \quad (11)$$

Besides, for ions having a charge $z = 1$, these individual diffusion coefficients D_i are such that:

$$D_i = \lambda\frac{RT}{f^2}, \quad (12)$$

where f is the Faraday constant, R the molar gas constant, T the absolute temperature and λ the equivalent ionic conductivity of the considered ion. Values of λ for K^+ and SCN^- in acetonitrile were taken from the literature [20], and the corresponding values of D_i and D_0 were easily calculated from Eqs. (12) and (11), respectively. Concerning γ-butyrolactone, no bibliographic data were found for λ. Consequently, the behaviours of ions having equivalent conductivities very close to those of K^+ on the one hand, and of SCN^- on the other hand, were compared in various solvents [21], and values of λ were roughly estimated from such comparisons. Moreover, the estimated values are in agreement with the conductivity χ of a dilute solution (5×10^{-5} mol l^{-1}) of KSCN in γ-butyrolactone. Indeed, one obtains $(\chi \times 1000)/(5 \times 10^{-5}) \approx \Sigma\lambda = 38.2$, while our estimations of λ_{K^+} and λ_{SCN^-} give $\Sigma\lambda \approx 42$. All the data concerning equivalent ionic conductivities, individual and overall diffusion coefficients are gathered in Table 3.

The formation factors of wetted materials are now calculated from Eq. (2) using the data of D and D_0 given in Tables 1 and 3, respectively. The results may be found in Table 4. As suspected above, the formation factors are much greater than in the case of dry materials. The tortuosities of the films impregnated with acetonitrile may also be derived from the porosities of these materials obtained in the previous subsection, see Table 4. However, such calculation is not possible in the case of γ-butyrolactone since the electrodes wetted with the latter behave like gels in which fluid flow does not occur. Hence, the porosity was not calculable from permeability measurements, and thus, the tortuositues are not known. Moreover, even if such a porosity was estimated, it would be very different from that of materials swelled by acetonitrile. Indeed, in the latter, a classical pore network is likely, i.e. having connected pores throughout which a fluid may flow. Besides, the same kind of pore structure as that of dry materials, i.e. capillary tubes being now much more tortuous than before, is assumed to hold. With γ-butyrolactone, the polymer swells until the ''macroscopic'' porosity vanishes. However, since the macromolecular network is now much less slack, diffusion seems to be only slightly hindered. These statements are supported by Table 4, in which it is seen that the values of F are in most cases only slightly greater with γ-butyrolactone than with

Table 4
Formation factors F of electrodes impregnated by acetonitrile and γ-butyrolactone

Sample	Acetonitrile			γ-Butyrolactone	
	F	τ	R_s (Ω cm^2)	F	R_s (Ω cm^2)
F_1	88.92	13.43	2.9	91.81	5.0
F_2	65.33	10.58	2.7	–	4.4
F_3	60.54	10.23	2.4	67.25	4.1
F_4	86.23	15.61	2.7	62.20	4.1
F_5	49.73	9.65	2.4	–	3.8
F_6	35.42	7.86	2.4	58.99	3.5

Tortuosities τ are calculated only if the porosities are known, i.e. in the case of films wetted by acetonitrile. The series resistances R_s of the corresponding supercapacitors based on these materials are also given.

acetonitrile. Additionally, it may be noticed that the series resistances follow the same behaviour.

3.3. Formation factors—series resistances relationships

The work described above, thus, allowed the derivation of the formation factors F in the polymeric matrices comprising various amounts of carbon grains. It should be emphasised again that such formation factors were measured with films being in a constrained state, and hence, are relevant of what really occurs in supercapacitors in actual working conditions. Finally, it is worth noting that the values of F widely vary from samples 1 to 6. This finding is in strong contrast with the compositions of the films. Indeed, the latter are such that both the carbon contents and the porosities are only slightly different from a sample to another (see Table 1). Therefore, it is clearly shown here that, for similar porous electrodes, the porous structure may be rather different. The latter, thus, depends on both the initial composition and the impregnating solvent.

The series resistances of supercapacitors based on films F_1–F_6 are plotted versus the formation factors of the electrodes in Fig. 10. It may be seen that a same kind of linear variation is obtained, whatever the solvent. Thus, despite the fact that surprisingly high formation factors were found for F_6 in the dry state and for F_4 impregnated with acetonitrile, the experimental points are shown to fall correctly into a line. It, thus, seems that, for given solvent, electrolyte and conducting filler, the smaller the formation factors, the smaller the series resistances. Since the range of composition of the samples is very narrow, the variations of series resistance undoubtedly originates from the formation factors of the films, and hence, from their tortuosities.

One striking feature is that the formation factors are not much different in electrodes impregnated with either acetonitrile or with γ-butyrolactone, while these solvents were shown to induce very different permeabilities. Since both solvents have similar relative dielectric constants, the differences between the observed R_s at a same value of F may be attributed to the different viscosities of these solvents. Consequently, obtaining a supercapacitor with a low series resistance is probably achieved with a solvent of low viscosity and high dielectric constant impregnating electrodes having straight pores. The latter condition is satisfied with a moderate content of filler dispersed into a porous matrix. However, lowering the volume fraction of carbon grains will also decrease the available surface area and, hence, the capacity of the device. Therefore, further studies are required in order to find the best compromise between high capacity and low series resistance.

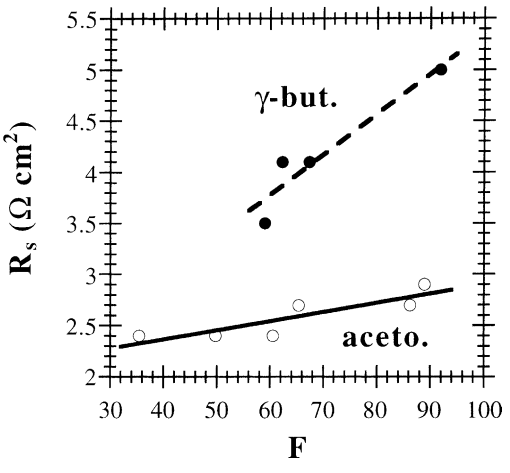

Fig. 10. Empirical correlation between formation factors F of porous electrodes impregnated with either acetonitrile or γ-butyrolactone and the series resistance (R_s) of actual supercapacitors based on these electrodes.

4. Conclusion

Porous electrodes designed for supercapacitors were investigated in this paper. The materials were made of a porous polymer matrix comprising active carbon grains. The porosities and the permeabilities of these materials were determined, and the pore structure was found to be correctly modelled by slightly tortuous capillary tubes.

Depending on the solvent with which the electrodes were impregnated, their permeabilities and, thus, their pore structure were found to be very different. The compositions investigated here swelled both in acetonitrile and γ-butyrolactone, which have the required characteristics to be used in supercapacitors. However, while the former solvent lead to materials in which the porosity was lowered but still effective for fluid flow, an almost non permeable polymeric gel was obtained with the latter.

It has been shown that the series resistances measured in supercapacitors based on such electrodes is a decreasing function of their porosities. However, the latter are not known for materials which swell as gels, as in the case of the present compositions impregnated with γ-butyrolactone. Thus, the formation factors F, being the ratios of the ionic conductivities of a given electrolyte to those of pore spaces saturated with the same electrolyte, were found to be very interesting parameters. Indeed, F expresses the relative easiness for ions to diffuse within a porous structure. For a given solvent, it was clearly shown that the greater is such easiness, the lower is the corresponding series resistance. Such a conclusion should be true in any other kind of porous polymeric composite used as electrode in double-layer supercapacitor, whatever its composition or chemical nature. However, more work is required to optimise the capacity of the supercapacitors, which may vary in the opposite direction to that of the series resistance.

Acknowledgements

This work was supported by a research agreement between the Laboratoire de Chimie du Solide Minéral,

UMR-CNRS 7555, Bolloré Technologies Ltd. and Elf Atochem. I. Rey, from Bolloré Technologies, is gratefully acknowledged for supplying the porous electrodes used all along the present work. The authors also wish to thank H. Lini, from CECA Group (France), for providing the mercury porosimetry data presented in this paper. Finally, one of us (F. Collas) acknowledges with thanks the financial support of Bolloré Technologies Ltd. all along his post-doctoral training course.

References

[1] B.E. Conway, Electrochemical Supercapacitors, Kluwer Academic Publishers/Plenum Press, Dordrecht/New York, 1999, pp. 335–452.
[2] L.M. Schwartz, N. Martys, D.P. Bentz, E.J. Garboczi, S. Torquato, Phys. Rev. E 48 (1993) 4584.
[3] A.B. Shelekhin, A.G. Dixon, Y.H. Ma, J. Membr. Sci. 83 (1993) 181.
[4] F. Collas, J.F. Marêché, A. Celzard, unpublished results.
[5] B. Lundberg, B. Sundqvist, J. Appl. Phys. 60 (1986) 1074.
[6] A.E. Scheidegger, The Physics of Flow Through Porous Media, 3rd Edition, University of Toronto Press, Toronto and Buffalo, 1974, p. 73.
[7] F.A.L. Dullien, Porous Media-Fluid Transport and Pore Structure, Academic Press, New York, 1979, pp. 79–81.
[8] Merck Databank Online: http://chemdat.merck.de.
[9] M. Ue, in: Proceedings of the 8th International Seminar on Double-Layer Capacitors and Similar Energy Storage Devices, Review of the Electrolyte Materials for Double-Layer Capacitors, Deerfield Beach, FL, December 1998.
[10] J. Van Brakel, S. Modry, M. Svata, Powder Technol. 29 (1981) 1.
[11] M. Sahimi, Applications of Percolation Theory, Taylor and Francis, Bristol, PA, 1994, pp. 15–16.
[12] A.J. Katz, A.H. Thompson, Phys. Rev. B 34 (1986) 8179.
[13] A.J. Katz, A.H. Thompson, J. Geophys. Res. 92 (1987) 599.
[14] P.G. de Gennes, E. Guyon, J. Méc. 17 (1978) 403.
[15] I. Chatzis, F.A.L. Dullien, J. Can. Pet. Technol. 16 (1977) 97.
[16] A.H. Thompson, A.J. Katz, R.A. Rashke, Phys. Rev. Lett. 58 (1987) 29.
[17] A. Celzard, J.F. Marêché, J. Phys.: Condens. Matter 13 (2001) 4387.
[18] P. Le Doussal, Phys. Rev. B 39 (1989) 4816.
[19] J.R. Banavar, M. Cieplak, D.L. Johnson, Phys. Rev. B 37 (1988) 7975.
[20] G.J. Janz, R.P.T. Tomkins, Nonaqueous Electrolytes Handbook, Vol. I, Academic Press, New York, London, 1972.
[21] M. Ue, J. Electrochem. Soc. 141 (1994) 3336.